

Real-time detection of probe loss in atomic force microscopy

Tathagata De, Pranav Agarwal, Deepak R. Sahoo, and Murti V. Salapaka^{a)}

Department of Electrical and Computer Engineering, Iowa State University, Ames, Iowa 50011

(Received 1 March 2006; accepted 16 August 2006; published online 28 September 2006)

In this letter, a real-time methodology is developed to determine regions of dynamic atomic force microscopy based image where the cantilever fails to be an effective probe of the sample. Conventional imaging signals such as the amplitude signal and the vertical piezoactuation signal cannot identify the areas of probe loss. It is experimentally demonstrated that probe-loss affected portion of the image can be unambiguously identified by a real-time signal called reliability index. Reliability index, apart from indicating the probe-loss affected regions, can be used to minimize probe-loss affected regions of the image, thus aiding high speed AFM applications. © 2006 American Institute of Physics. [DOI: 10.1063/1.2357876]

In dynamic mode operation of the atomic force microscope (AFM), the base of the cantilever is forced sinusoidally near the first modal frequency of the cantilever. When the cantilever tip interacts with the sample, the tip-sample interaction force changes the deflection of cantilever. The sample features are gleaned from the cantilever deflection signal. In amplitude modulated AFM operation,¹ the amplitude of the first harmonic component of the cantilever oscillation is regulated at a desired set point by regulating the vertical position of the sample.

In tapping mode AFM (TM-AFM), vertical piezoactuation signal that regulates cantilever-sample separation is interpreted as the image of the sample.¹ In a less prevalent mode, namely, error signal mode (ESM) imaging, feedback loop serves as a high-pass filter and error signal that is the difference between the cantilever amplitude and the setpoint amplitude² forms the image of the sample.

In AFM, the cantilever is the main probe for sample topography and therefore when the cantilever loses its interaction with the sample, it is not possible to glean information about the sample from the cantilever deflection. We will term the condition of the cantilever not being affected by the sample as the probe-loss condition.

Areas affected by probe loss scales linearly with imaging speed and therefore probe loss is a factor that limits the maximum achievable scan rate. This effect is also known as “parachuting effect” of cantilever.³ Issue of low imaging bandwidth and probe loss due to transient response of probe has been partially addressed by active Q control of probe.^{4,5} Dynamic proportional-integral-derivative (PID) control for z feedback loop is also used to reduce areas affected by parachuting effect.⁶ All prior works have attempted to address the issue of probe ineffectiveness without identifying the occurrence of probe loss and therefore these methods treat regions of probe loss and regions not affected by probe loss in the same manner. This aspect of existing methods has the adverse effect of compromising image quality in the regions of the image where probe loss is not an issue.

Traditionally employed signals, e.g., amplitude or vertical piezoactuation signal, that estimate the sample topography are not characteristically different in the presence or absence of the probe-loss condition. These signals, therefore,

cannot be used to identify or correct probe-loss condition to improve imaging speed. Real-time identification of probe loss enables, in contrast to existing methods, the design of corrective action that discriminates between the probe-loss affected regions from the probe-loss unaffected regions. Vulnerability of dynamic mode AFM operation to probe loss is evident in Figs. 1(a) and 1(b) that present images of uniform rectangular and triangular sample profiles, respectively. Samples were scanned at 20 Hz spatial frequency by a Multimode AFM, manufactured by Veeco Metrology Inc. A silicon cantilever with resonant frequency $f_0=71.3$ kHz and quality factor $Q=124$ was used in these scans.

Figure 1 demonstrates experimentally that similar amplitude profiles can result when the cantilever is probing two different sample profiles. In Fig. 1(a), at p the sample has a step feature where the cantilever stops interacting with the sample leading to probe loss. The amplitude increases slowly until it attains its free resonant amplitude at q . In Fig. 1(b) the cantilever probe is active throughout the imaging region and the image is not affected by probe loss. Amplitude profiles are similar between p and q and between \tilde{p} and \tilde{q} , even though two different samples are being probed. Therefore the amplitude or the error signal does not provide a reliable measure of probe loss. Figures 2(a) and 2(b) show tapping mode images of rectangular and triangular profiles at 20 Hz, respectively. In Fig. 2(a) height profile displays a smooth transition instead of a sharp edge. The height profile generated while going down the ramp between \tilde{p} and \tilde{q} in Fig. 2(b) is similar to probe-loss region between \hat{p} and \hat{q} in Fig. 2(a). It demonstrates that vertical actuation signal is also not well suited as a measure of probe loss.

The area affected by probe loss primarily depends on the quality factor of the cantilever and scales linearly with the scan speed. Also, high quality factors are desirable as they aid imaging with higher resolution. Thus most existing methods for high speed imaging have to perform a trade-off between resolution and bandwidth; low quality factors lead to smaller probe loss but lower resolution imaging and vice versa. It is also evident that probe-loss affected areas lead to spurious interpretation of the image (areas between p and q and \hat{p} and \hat{q}). There is thus an evident need to identify the probe-loss scenario so that the AFM data can be interpreted correctly and subsequently used to correct for probe loss. In this letter, a method for detecting probe loss during imaging is presented. It is also shown that the method can detect the

^{a)}Electronic mail: murti@iastate.edu

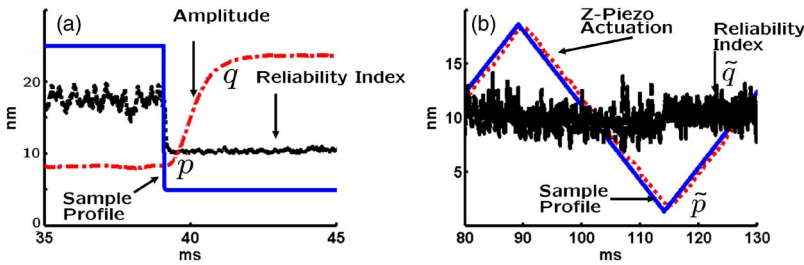


FIG. 1. (Color online) Shows the experimentally obtained amplitude signal during ESM-AFM imaging. (a) and (b) shows the amplitude profile and reliability index when imaging rectangular and triangular samples, respectively.

probe loss sufficiently fast that enables its use in real time. This real-time detection of probe loss can be used to minimize probe-loss affected areas by taking corrective action of the AFM operation by changing the controller gains of the scanner and the cantilever in real time.

Near its first resonant frequency, the cantilever can be modeled as a spring-mass-damper system. In the absence of the sample, cantilever-tip dynamics is described by the following equation of motion:

$$\ddot{p} + \frac{\omega_0}{Q}\dot{p} + \omega_0^2 p = g(t) + \eta(t); \quad [p(0), \dot{p}(0)], \quad (1)$$

where $\omega_0 = 2\pi f_0$ is the first resonant frequency of the cantilever, Q is the quality factor of the cantilever, p is the cantilever deflection, $p(0)$ is the initial tip deflection, $\dot{p}(0)$ is the initial tip velocity, $g(t)$ is the dither force, and $\eta(t)$ is the thermal noise. Tip position of the cantilever is detected by the photodiode that generates voltage $y = Sp + v$, where S is the photodiode sensitivity and v is the measurement noise. With these parameters, the cantilever dynamics can be mimicked by an analog circuit or by a fast digital circuit, called the observer of the cantilever, that outputs a voltage \hat{y} , given by

$$\ddot{\hat{y}} + \frac{\omega_0}{Q}\dot{\hat{y}} + \omega_0^2 \hat{y} = g(t), \quad [\hat{y}(0), \dot{\hat{y}}(0)], \quad (2)$$

where $\dot{\hat{y}}(0)$ and $\hat{y}(0)$ form the initial conditions of the observer state (see Fig. 3).

In the absence of the sample, in steady state, after the initial condition mismatch between the cantilever state and the observer state has died out, the error e is near zero as the cantilever dynamics given by Eq. (1), and the observer dynamics given by Eq. (2) are identical. The remnant mismatch in steady state is due to photodiode noise and the thermal noise that affects the measured cantilever deflection without affecting the observer circuit. In the presence of the sample, the cantilever behaves as a modified cantilever with changed quality factor and changed resonant frequency. If the sample force is given by $h(p, \dot{p})$, the estimates of the equivalent cantilever frequency and the quality factor are given by:^{7,8}

$$\omega_0'^2 = \omega_0^2 + \frac{2}{a} \frac{1}{2\pi} \int_0^{2\pi} h(a \cos \psi, -a\omega \sin \psi) \cos \psi d\psi \quad (3)$$

and

$$\frac{\omega_0'}{Q'} = \frac{\omega_0}{Q} + \left(\frac{1}{a\omega} \frac{1}{\pi} \int_0^{2\pi} h(a \cos \psi, -a\omega \sin \psi) \sin \psi d\psi \right), \quad (4)$$

respectively, where a is the steady state amplitude of the cantilever in the presence of the sample. Thus the cantilever behavior under the sample presence is given by

$$\ddot{p} + \frac{\omega_0'}{Q'}\dot{p} + \omega_0'^2 p = g(t) + \eta(t). \quad (5)$$

Note that the observer still behaves according to Eq. (2), thus the difference between the observer and the cantilever is due to the change in the model parameters that do not decay with time. Thus the persistent error between the observer and the cantilever dynamics is utilized to provide a signal that indicates presence of the sample. This is unlike and in contrast to the change due to initial condition mismatch that is used to transiently detect the sample presence in Ref. 9

The mismatch $e := y - \hat{y}$ between the dynamics of Eqs. (1) and (2) in steady state provides a measure of sample presence and therefore for the no probe-loss region. However, to be useful in real time, this error should decay at a high rate when the sample is not interacting with the cantilever. It can be shown that the error dynamics, caused by initial condition mismatch between Eqs. (1) and (2), once the cantilever comes off the sample decays on a time scale proportional to $1/Q$ which is unacceptably slow. The drawback of the observer [Eq. (2)] can be alleviated by implementing a new scheme, where a correction signal ($u(t) = [l_1 l_2]^T [e(t) \dot{e}(t)]$) is added to $g(t)$ and given as input to the observer circuit to make the observer track the cantilever faster (effectively decoupled from Q), where $e := y - \hat{y}$ (called *innovation* here after) is the difference between the cantilever deflection and the observer estimated deflection. $L = [l_1 l_2]^T$ is the gain of the observer. When the cantilever is not interacting with the sample, innovation follows the equation:

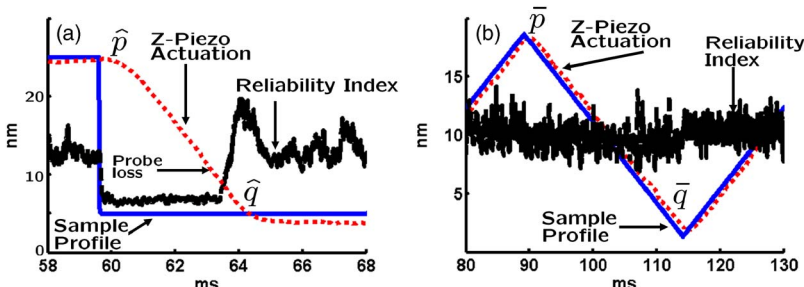


FIG. 2. (Color online) Shows the experimental vertical piezoactuation signals during TM-AFM imaging. (a) and (b) shows the height profile based on vertical actuation signal when imaging rectangular and triangular samples, respectively.

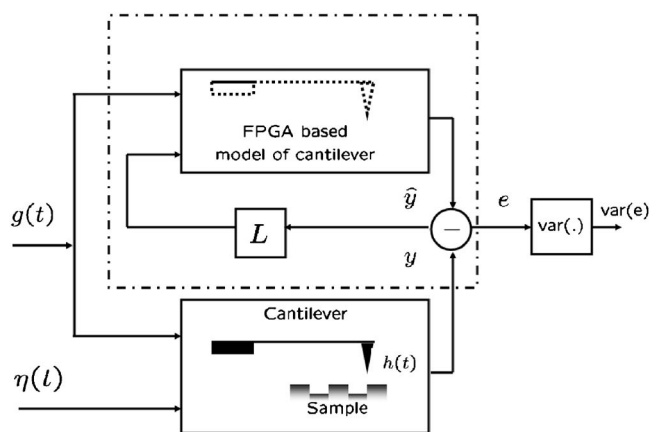


FIG. 3. Model of the cantilever near its resonant frequency is mimicked by a high speed (10 MHz) electrical circuit implemented on Xilinx Virtex II Pro XC2VP30 FPGA. Nonzero value of e arises from initial condition mismatch, $\eta(t)$, and $h(p, \dot{p})$.

$$\ddot{e} + \left(\frac{\omega_0}{Q} + l_1 \right) \dot{e} + \left(\omega_0^2 + \frac{\omega_0}{Q} l_1 + l_2 \right) e = \eta - l_1 \dot{v} - \left(\frac{\omega_0}{Q} + l_1 \right) v; \quad [e(0), \dot{e}(0)]. \quad (6)$$

It can be shown that the effect of initial condition mismatch in innovation signal decays within a couple of cycles. The new innovation signal's capability of yielding a high value when interacting with the sample and the observer's ability to erase the effects of the sample on the innovation in a couple of cycles when the sample is absent make it possible for real-time detection of probe loss. To utilize this property of innovation, a parameter, called reliability index (N sample variance of innovation, where N is chosen according to observer bandwidth, false alarm, and miss probability in probe-loss detection), is derived which maintains a high value when the tip is interacting with sample and drops to near zero value otherwise. In Fig. 1(b), it is evident that reliability index increases monotonically with decreasing tip-sample separation. This result agrees with the intuition that smaller tip-sample separation leads to greater changes to equivalent resonance frequency and equivalent damping, thereby leading to greater model mismatch between observer and cantilever dynamics. This property of reliability index immediately lends itself for the design of thresholds for detection of probe loss.

In Fig. 1(a) reliability index drops below threshold unit within couple of cycles as it comes off the step indicating detection of probe-loss condition. As a comparison, amplitude signal takes approximately 155 cycles to indicate that cantilever is no longer interacting with the sample. In Fig. 2(a), reliability index is used for the detection of probe loss and areas requiring gain and Q adjustment, which is not possible using traditional imaging parameters such as amplitude (A), error signal ($A - A_{\text{setpoint}}$) or vertical piezoactuation signal. Figure 2(a) shows that when the cantilever comes off the step at \hat{p} the reliability index drops only in a couple of cantilever oscillations, indicating probe loss between \hat{p} and \hat{q} . At \hat{q} , height image becomes the true reflection of sample profile

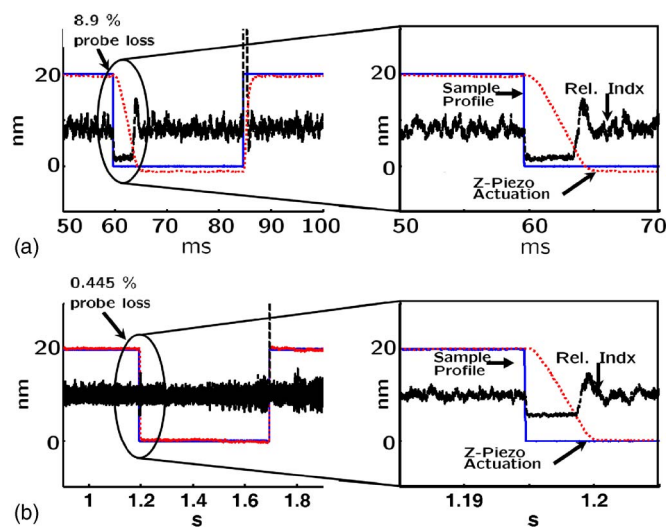


FIG. 4. (Color online) In (a) and (b), a rectangular profile is imaged at 20 and 1 Hz, respectively.

and reliability index jumps above threshold, indicating the end of probe-loss condition. In Fig. 2(b) the reliability index stays above the threshold indicating that there is no probe loss. It is to be noted that at lower scan rates, effect of probe loss is not so prominent, it is present for exact same duration as for any other rate. At 20 Hz scan rate 8.9% area contains spurious height profile as compared to 0.445% at 1 Hz scan rate. Even though, probe loss is less prominent in Fig. 4(b), it is present for the same duration (4.45 ms), as in Fig. 4(a). The number of cycles of probe loss is determined largely by the quality factor Q of the cantilever and is independent of the scan rate. However, the fraction of the spurious image increases linearly with respect to scan speed that is particularly detrimental to high speed imaging applications.

In this letter, reliability index is presented as a fast real-time quantitative measure to detect probe loss. When used in conjunction to existing technologies such as Q control and dynamic PID control, this method may increase imaging bandwidth. This letter further demonstrates the effectiveness of observer based techniques in AFM.^{9,10}

This work was supported by the NSF Grant No. ECS0601571 to one of the authors (M.V.S.).

- ¹G. Binnig, C. F. Quate, and C. Gerber, *Phys. Rev. Lett.* **56**, 930 (1986).
- ²C. A. Putman, K. O. Werf, B. G. Grooth, N. F. Hulst, F. Niek, J. Greve, and P. K. Hansma, *Proc. SPIE* **1639**, 198 (1992).
- ³M. C. Strus, A. Raman, C. S. Han, and C. V. Nguyen, *Nanotechnology* **16**, 2482 (2005).
- ⁴T. Sulchek, G. G. Yaralioglu, C. F. Quate, and S. C. Minne, *Rev. Sci. Instrum.* **73**, 2928 (2002).
- ⁵T. Sulchek, R. Hsieh, J. D. Adams, G. G. Yaralioglu, S. C. Minne, C. F. Quate, J. P. Cleveland, A. Atalar, and D. M. Adderton, *Appl. Phys. Lett.* **76**, 1473 (2000).
- ⁶T. Ando, T. Uchihashi, N. Kodera, A. Miyagi, R. Nakakita, H. Yamashita, and M. Sakashita, *Jpn. J. Appl. Phys., Part 1* **45**, 1897 (2006).
- ⁷M. Gauthier, N. Sasaki, and M. Tsukada, *Phys. Rev. B* **64**, 085409 (2001).
- ⁸Yu. A. Mitropolsky and N. V. Dao, *Applied Asymptotic Methods in Non-linear Oscillations* (Kluwer, Dordrecht, 1997), pp. 106–117.
- ⁹D. R. Sahoo, A. Sebastian, and M. V. Salapaka, *Appl. Phys. Lett.* **83**, 5521 (2003).
- ¹⁰S. Salapaka, T. De, and A. Sebastian, *Appl. Phys. Lett.* **87**, 053112 (2005).